A Fast Approach for No-Reference Image Sharpness Assessment Based on Maximum Local Variation

Khosro Bahrami, *Student Member, IEEE*, and Alex C. Kot, *Fellow, IEEE*

Abstract—**This letter proposes a simple and fast approach for no-reference image sharpness quality assessment. In this proposal, we define the maximum local variation (MLV) of each pixel as the maximum intensity variation of the pixel with respect to its 8-neighbors. The MLV distribution of the pixels is an indicative of sharpness. We use standard deviation of the MLV distribution as a feature to measure sharpness. Since high variations in the pixel intensities is a better indicator of the sharpness than low variations, the MLV of the pixels are subjected to a weighting scheme in such a way that heavier weights are assigned to greater MLVs to make the tail end of MLV distribution thicker. The weighting leads to an improvement of the MLV distribution to be more discriminative for different blur degrees. Finally, the standard deviation of the weighted MLV distribution is used as a metric to measure sharpness. The proposed approach has a very low computational complexity and the performance analysis shows that our approach outperforms the state-of-the-art techniques in terms of correlation with human vision system on several commonly used databases.**

Index Terms—**Human vision system, image quality assessment, maximum local variation, sharpness/blurriness assessment.**

I. INTRODUCTION

SHARPNESS assessment of digital images is important in many modern image processing systems. The objective of sharpness assessment is to evaluate the image quality in such a way that it is consistent with the human vision perception.

Based on the availability of the reference image, the image quality assessment (IQA) approaches are classified into full-reference (FR) [1]–[5], reduced-reference (RR) [6]–[9], and no-reference (NR) [10]–[30]. In this letter, we propose a simple and fast approach for NR image sharpness assessment which is suitable for online applications. Our work is motivated by the fact that maximum variations in the pixel intensity and the regions with the highest sharpness are highly correlated with the human sharpness perception. Our work has the following contributions: (1) We propose a technique which has a very low computational time compared with some existing methods. (2) Our technique outperforms the performance of the state-of-the-art approaches.

Various approaches have been introduced to measure the image sharpness in the literature which can be categorized into two categories, namely spatial and transform domain. The first category focuses on the image content variation in the spatial domain such as the spread of edges and texture. Ferzli *et al.* [11] used edge width with a concept called just noticeable blur (JNB). Narvekar *et al.* [12] proposed an approach named cumulative probability of blur detection (CPBD). The work proposed by Vu *et al.* [14] called S3 incorporates spatial total variation (TV) and local spectral information. In another approach, Mittal *et al.* [17] proposed a Blind/Referenceless Image Spatial QUality Evaluator (BRISQUE) which utilizes the natural scene statistic of local luminance coefficients. The works in [18]–[20] evaluate some functions for focus and sharpness measurement. Among various functions discussed, two functions called Thresholded Absolute Gradient (TAG) and Squared Gradient (SG) are defined as the summation of the vertical and horizontal pixel differentiations when they are larger than a threshold. However, these approaches capture the variations only in horizontal, vertical or a specific direction.

The second category examines the image in the transform domains. Hassen *et al.* [26] proposed a metric based on local phase coherence (LPC). There are other approaches that measure the image sharpness based on the distribution of transform coefficients. For instance, Moorthy *et al.* [28] proposed an approach called Distortion Identification-based Image INtegrity and Verity Evaluation (DIIVINE) which deploys natural scene statistics of image wavelet coefficients. Saad *et al.* [29], [30] developed a method named BLInd Image Notator using DCT Statistics (BLIINDS) based on the natural scene statistics of block DCT coefficients. However, these operations done in transform domain are time consuming which are not suitable for real time application.

The rest of this letter is organized as follows. In Section II, we propose the concept of the maximum local variation. The method for image sharpness assessment is proposed in Section III. Experimental results and discussions are given in Section IV. Section V concludes the letter.

II. MAXIMUM LOCAL VARIATION

In this section, we propose a novel metric called Maximum Local Variation (MLV) for sharpness assessment. Variations in the pixel values are an indication of image sharpness. Edges and textures contain lots of pixel variations that create impacts on the perceived sharpness by human vision system. However, employing the high variations in the pixel intensities is a better indicator of the sharpness than low variations. Capturing the intensity variations using the TV have been studied in the previous

Fig. 1. The value of normalized TV and MLV of the center pixel $I_{i,j}$ in four 3×3 blocks. (a) $\Upsilon_n(I_{i,j}) = 0$, $\psi_n(I_{i,j}) = 0$; (b) $\Upsilon_n(I_{i,j}) = 0.10$, $\psi_n(I_{i,j}) = 0.21$; (c) $\Upsilon_n(I_{i,j}) = 0.5$, $\psi_n(I_{i,j}) = 1$; (d) $\Upsilon_n(I_{i,j}) = 1$, $\psi_n(I_{i,j}) = 1$.

Fig. 2. MLV map. (a) an image (b) MLV map where the brighter pixels show larger MLV than the dark pixels.

work [14] for sharpness assessment. In the TV, all variations of the pixel values with respect to its 8-neighbors are employed to measure the sharpness given by

$$\Upsilon(I_{i,j}) = \sum_{x=i-1}^{i+1} \sum_{y=j-1}^{j+1} |I_{i,j} - I_{x,y}| \tag{1}$$

where $I_{i,j}$ is the pixel at location (i,j) in the image I, $I_{x,y}$ indicates one of the 8-neighbors of $I_{i,j}$, and $\Upsilon(I_{i,j})$ computes the TV of $I_{i,j}$ using l_1 norm distance. However, there are other ways to define TV with 2, 3 or 4 neighbors, or l_2 norm [31].

Different from the TV, we define MLV of a pixel $I_{i,j}$ (a pixel at location (i,j) of the image I) as the maximum variation between the intensity of $I_{i,j}$ with respect to its 8-neighbor pixels given by

$$\psi(I_{i,j}) = \{\max |I_{i,j} - I_{x,y}| | x = i-1, i, i+1 \; y = j-1, j, j+1\} \tag{2}$$

where $I_{x,y}$ $(i-1 \le x \le i+1, j-1 \le y \le j+1)$ are the 8-neighbors of $I_{i,j}$. Our study on the intensity variation measurements shows that MLV captures the variations better than TV. In the gray scale images, MLV changes in the range of 0–255. The value of 0 means there is no variation between a pixel and its 8-neighbors while the value of 255 shows the highest variation between the pixel and its 8-neighbors. The TV is changed in the range of $0 - (8 \times 255)$ in the case of using l_1 norm distance with 8-neighbors.

To get a better insight, we use four 3×3 blocks including a pixel $I_{i,j}$ and its 8-neighbors shown in Fig. 1 as an example. The pixel $I_{i,j}$ in (a) has no variation with respect to its 8-neighbors. The intensity variation of the block in (c) is larger than (b), and the pixel $I_{i,j}$ in (d) has the maximum variation with respect to its 8-neighbors. In Fig. 1(a), $\Upsilon(I_{i,j}) = 0$ and $\psi(I_{i,j}) = 0$ means $I_{i,j}$ has no variation with respect to its 8-neighbors. In Fig. 1(d), $\Upsilon(I_{i,j}) = 8 \times 255$ and $\psi(I_{i,j}) = 255$ shows that $I_{i,j}$ has the maximum variation with respect to its 8-neighbors. To have a fair comparison, the values of TV and MLV are normalized to [0 1] to set $\Upsilon_n(I_{i,j}) = 0$, and $\psi_n(I_{i,j}) = 0$ for $I_{i,j}$ in (a), and $\Upsilon_n(I_{i,j}) = 1$, $\psi_n(I_{i,j}) = 1$ for $I_{i,j}$ in (d) where $\Upsilon_n(.)$ and $\psi_n(.)$ are the normalized $\Upsilon(.)$ and $\psi(.)$, respectively. For Fig. 1(c), $\Upsilon_n(I_{i,j}) = 0.10$, $\psi_n(I_{i,j}) = 0.21$, and for Fig. 1(b), $\Upsilon_n(I_{i,j}) = 0.5$, $\psi_n(I_{i,j}) = 1$, shows that the MLV due to the larger $\psi_n(I_{i,j})$ than $\Upsilon_n(I_{i,j})$, can capture the small and large pixels variations better than TV.

III. PROPOSED METHOD

The proposed method for image sharpness assessment are explained in details in the following sections.

A. Maximum Local Variations Map Generation

Given a color image G of size $M \times N$, we first convert it to the gray scale image I. Then, for each pixel $I_{i,j}$ at location (i,j), we consider a 3×3 block $B_{i,j}$ including the 8-neighbor pixels of $I_{i,j}$, where $1 \le i \le M$ and $1 \le j \le N$. The MLV of all pixels $I_{i,j}$ are calculated using Eq. (2) to generate the MLV map $\Psi(I)$ of the image I given by

$$\Psi(I) = \begin{pmatrix} \psi(I_{1,1}) & \cdots & \psi(I_{1,N}) \\ \vdots & \ddots & \vdots \\ \psi(I_{M,1}) & \cdots & \psi(I_{M,N}) \end{pmatrix} \tag{3}$$

Fig. 2 shows an image and its corresponding MLV map. Dark color in the map shows pixels with small MLV, while bright color indicates pixels with larger MLV.

B. Maximum Local Variations Distribution

Our study on the statistics of MLV shows that the distribution of MLV is affected by the content and the blurriness of the image. We observe that the distribution in the texture region with low variation is closer to Gaussian, whereas the regions with high MLV edges and blank content have hyper-laplacian distribution. Fig. 3 shows two sharp images in (a) and (b) and the corresponding blurred versions in (e) and (f). The image in (a) has lots of regions with small as well as large MLV, whereas the one in (b) includes the regions with less variations than (a). The MLV distributions of (a) and (b) are shown in Fig. 3(c) and (d), respectively. By increasing the blur degree in the images, the MLV distribution of the blurred images shown in (g) and (h) tends to drop in the number of the large MLV values.

To use the statistics of MLV distribution for sharpness assessment, we parameterize the MLV distribution with Generalized Gaussian Distribution (GGD) used in [17], [28], [30], the general form of Gaussian, laplacian and hyper-laplacian distributions, given by

$$f(\Psi(I); \mu, \gamma, \sigma) = \left(\frac{\gamma}{2\sigma\Gamma\left(\frac{1}{\gamma}\right)\sqrt{\frac{\Gamma\left(\frac{1}{\gamma}\right)}{\Gamma\left(\frac{3}{\gamma}\right)}}} \right) e^{-\left(\frac{\Psi(I)-\mu}{\sigma\sqrt{\frac{\Gamma\left(\frac{1}{\gamma}\right)}{\Gamma\left(\frac{3}{\gamma}\right)}}} \right)^{\gamma}} \tag{4}$$

where μ is the mean, σ is the standard deviation, γ is the shape-parameter, and $\Gamma(.)$ is the gamma function. The standard deviation σ decreases by increasing the blurriness which can be used
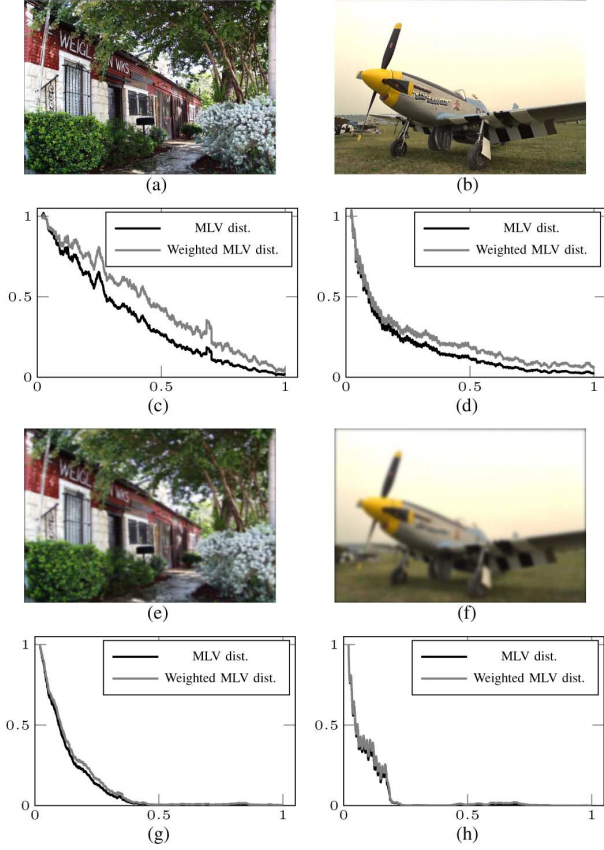
Fig. 3. (a) a sharp image with low and high variation regions; (b) a sharp image with blank, low and high variation regions; (c) and (d) MLV vs. weighted MLV distribution of (a) and (b), respectively; (e) and (f) blurred version of (a) and (b), respectively; (g) and (h) MLV vs. weighted MLV distribution of (e) and (f), respectively.

as the sharpness measurement metric. Since the human vision system is more sensitive to higher variations regions, we refine in the next step the MLV map by assigning different weights to the pixels with various MLV values which reshape the MLV distribution to model the sharpness non-linearity.

C. Maximum Local Variations Content-Based Weighting

The distribution statistics of the images in Fig. 3 reveal that the tail end of the distribution discriminates the blur degree differences. The pixels with large MLV have more influences in the sharpness assessment. By changing the distribution in such a way that the tail part becomes heavy, the distribution can be used to evaluate the sharpness more effectively. This can be done by assigning higher weights to the larger MLV pixels by generating the weighted MLV map $\Psi_w(I)$ below

$$\Psi_w(I) = \begin{pmatrix} w_{1,1}\psi(I_{1,1}) & \cdots & w_{1,N}\psi(I_{1,N}) \\ \vdots & \ddots & \vdots \\ w_{M,1}\psi(I_{M,1}) & \cdots & w_{M,N}\psi(I_{M,N}) \end{pmatrix} \quad (5)$$

where weights $w_{i,j}$ are defined using exponential function $w_{i,j} = e^{\eta_{i,j}}$ and $\eta_{i,j}$ is the rank of $\psi(I_{i,j})$ when sorted in ascending order from 0 to 1. By choosing weight as an exponential function, the measured sharpness is well correlated with human vision based on sharpest region in the image [26]. In addition, exponential is better than linear function since it gives

higher weight to the pixels with larger MLV. After weighting, the tail end of distribution of sharp images in Fig. 3(c) and (d) become thicker while the tail end of distribution of the blurred images in Fig. 3(g) and (h) have very small changes. Therefore, the tail end of the weighted MLV distributions can work better in sharpness discriminative than the tail end of the MLV distributions. The GGD distribution of the weighted MLV is driven by replacing $\Psi(I)$ with $\Psi_w(I)$ in Eq. (4). Finally, standard deviation of the weighted MLV distribution is used as the metric to measure sharpness calculated using the moment matching method in [32].

IV. EXPERIMENTAL RESULTS AND DISCUSSION

In this section, we compare the performance of our technique with the existing state-of-the-art NR image sharpness methods like TAG [19], SG [19], CPBD [12], DIIVINE [28], BLIINDS [30], BRISQUE [17], S3 [14] and LPC-SI [26] using LIVE [33], TID2008 [34], CSIQ [35] and IVC [36] databases. The LIVE, TID2008, CSIQ and IVC databases have 174, 100, 150 and 20 images, respectively.

We use five criteria to compare the performance of these methods including pearson Correlation Coefficient (CC), Spearman Rank-Order Correlation Coefficient (SROCC), Root Mean Square Error (RMSE), Mean Absolute Error (MAE) and Outlier Ratio (OR). High values for CC, SROCC and low values for RMSE, MAE and OR indicate good performance in terms of correlation with human vision system [37].

Table I compares the performance of our technique and the previous methods on LIVE, TID2008, CSIQ and IVC databases. For TAG [19] and SG [19], we consider the maximum value of the horizontal and vertical gradients, claimed by the author that improves the result significantly. We report our result and LPC-SI with/without weighting scheme to evaluate the contribution of the weighting. For LIVE database, Our technique demonstrates excellent performance among all methods. For TID2008, except MAE and OR, our technique are the best among all methods. For CSIQ database, except CC, our performance shows better results. For IVC, our technique shows the best performance among all.

Fig. 4 shows the scatter plots of the subjective scores of LIVE, TID2008, CSIQ and IVC databases versus objective scores of S3, LPC-SI and our technique after nonlinear mapping. Our technique shows less biasness in subjective versus objective scoring for these uncorrelated images when compared with the previous methods. For example, the scatter plot of our technique for CSIQ database in Fig. 4(k) shows a better spread along the diagonal line.

Since our technique works in spatial domain without any complex mathematical operation or transformation, the computational complexity is low. The main computational cost of our technique is determined by calculation of MLV of the pixels and parameters estimation of the MLV distribution which are linear with respect to the number of pixels n in the image and is in the order of $O(n)$. BRISQUE and CPBD have the computational complexity in the order of $O(n)$. In BRISQUE, the complexity is determined by two main tasks including 36 features extraction in spatial domain and 5 times GGD parameters estimation [17]. The complexity of CPBD is identified by edge detection
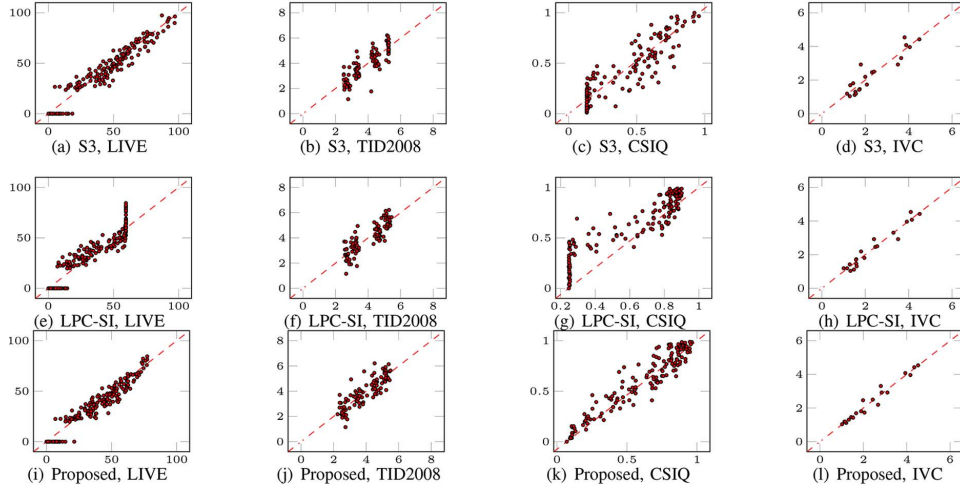
Fig. 4. Scatter plots of objective scores generated by S3 [14], LPC-SI [26] and our technique versus subjective scores reported by LIVE, TID2008, CSIQ and IVC databases after nonlinear mapping, where each dot represents one image.

TABLE I
COMPARISON OF OUR PROPOSED TECHNIQUE AND PREVIOUS WORKS ON LIVE, TID2008, CSIQ AND IVC DATABASES

Approach	CC	SROCC	RMSE	MAE	OR
LIVE database [33]					
TAG [19]	0.8850	0.8810	10.1249	7.9684	0.2241
SG [19]	0.8755	0.8652	10.5093	8.4463	0.2414
CBPD [12]	0.9107	0.9437	8.9857	6.8869	0.1609
DIIVINE [28]	used LIVE for training				
BLIINDS [30]	used LIVE for training				
BRISQUE [17]	used LIVE for training				
S3 [14]	0.9537	**0.9645**	8.1235	5.1320	0.1090
LPC-SI [26] w/o weighting	0.8569	0.8886	11.2119	8.9590	0.2931
LPC-SI [26] w weighting	0.9204	**0.9594**	8.5061	6.8987	0.1522
Proposed w/o weighting	0.9383	0.9378	7.5222	5.9220	0.0920
Proposed w weighting	**0.9590**	0.9566	**6.1676**	**4.8928**	**0.0517**
TID2008 database [34]					
Approach	CC	SROCC	RMSE	MAE	OR
TAG [19]	0.7449	0.7421	0.7829	0.6120	0.6800
SG [19]	0.7150	0.7153	0.8202	0.6366	0.6800
CBPD [12]	0.8316	0.8406	0.6438	0.5019	0.6500
DIIVINE [28]	0.8429	0.8322	0.6655	0.5031	0.6302
BLIINDS [30]	0.8415	0.8387	0.6339	**0.4010**	**0.5200**
BRISQUE [17]	0.8044	0.7989	0.6972	0.5059	0.6200
S3 [14]	0.8492	0.8327	0.6195	0.4790	0.6200
LPC-SI [26] w/o weighting	0.7424	0.7188	0.7862	0.6306	0.7000
LPC-SI [26] w weighting	0.8574	0.8531	0.6040	0.4856	0.6800
Proposed w/o weighting	0.8113	0.8117	0.6861	0.5313	0.6600
Proposed w weighting	**0.8585**	**0.8548**	**0.6018**	0.4675	0.6100
CSIQ database [35]					
Approach	CC	SROCC	RMSE	MAE	OR
TAG [19]	0.8352	0.8015	0.1576	0.1217	0.3867
SG [19]	0.8027	0.7957	0.1709	0.1308	0.4200
CBPD [12]	0.8820	0.8860	0.1349	0.1245	0.3730
DIIVINE [28]	0.8912	0.8930	0.1132	0.0951	0.2653
BLIINDS [30]	**0.9102**	0.8915	0.1187	0.0943	0.2867
BRISQUE [17]	**0.9274**	0.9025	0.1072	0.0822	0.2400
S3 [14]	0.9035	0.9017	0.1228	0.0996	0.3400
LPC-SI [26] w/o weighting	0.8892	0.8379	0.1311	0.1057	0.3200
LPC-SI [26] w weighting	0.9061	0.9071	0.1151	0.0927	0.2733
Proposed w/o weighting	0.8942	0.8498	0.1283	0.0976	0.3000
Proposed w weighting	0.9069	**0.9247**	**0.1069**	**0.0749**	**0.1933**
IVC database [36]					
Approach	CC	SROCC	RMSE	MAE	
TAG [19]	0.9231	0.9135	0.4387	0.3079	
SG [19]	0.7175	0.6388	0.7952	0.6130	
CBPD [12]	0.8865	0.8404	0.6629	0.5126	
DIIVINE [28]	0.8012	0.7984	0.5767	0.4325	
BLIINDS [30]	0.7837	0.5312	0.5893	0.4444	
BRISQUE [17]	0.8515	0.8239	0.4510	0.3775	
S3 [14]	0.9333	0.8916	0.4099	0.3266	
LPC-SI [26] w/o weighting	0.9116	0.8269	0.4693	0.3894	
LPC-SI [26] w weighting	0.9726	0.9398	0.2653	0.2017	
Proposed w/o weighting	0.9699	0.9624	0.2779	0.2038	
Proposed w weighting	**0.9812**	**0.9767**	**0.2203**	**0.1514**	

TABLE II
COMPARISON OF MEAN COMPUTATIONAL TIME OF METHODS IN GENERATING SHARPNESS SCORE OF 200 IMAGES WITH SIZE OF 3264×2448

Approach	CPBD [12]	S3 [14]	BLIINDS [30]	DIVIINE [28]	BRISQUE [17]	LPC-SI [26]	Proposed (MLV)
Time (sec)	8.7	367.6	910.4	470.2	2.3	19.5	**1.6**

computation similarly to the 2D-FFT [30]. The computational complexity of DIVIINE [28] is determined by complexity of wavelet transform which is in the order of $O(n \log(n))$ and parameters estimation of GGD.

We compare the mean runtime of seven sharpness measurement methods applied to 200 images with size of 3264×2448 from Google web site. This test is performed on a PC with Intel Core i5 CPU at 3.20 GHz, 8 GB RAM, Windows 7 64-bit, and Matlab 7.11. The results are summarized in Table. II. The slowest methods are BLIINDS, DIIVINE, LPC-SI and S3. The CPBD, BRISQUE and our technique are the most competitive approaches. Among all, our method with 1.6 seconds has the lowest computational time.

V. CONCLUSIONS

In this letter, we proposed a simple and fast technique for image sharpness assessment based on the maximum local variation (MLV). The MLV of each pixel is calculated by finding the maximum of the intensity variation with respect to its 8-neighbors. We showed that the MLV of the pixels capture the high variations in the pixels intensity. Since the human vision system is more sensitive to higher variations regions, the MLV of the pixels are subjected to a weighting scheme to make the tail end of MLV distribution thicker. Finally, the standard deviation of the weighted MLV distribution is used as a feature to measure image sharpness. Experimental results revealed that our technique outperforms the performance of state-of-the-art methods on LIVE, TID2008, CSIQ and IVC databases in terms of correlation with the human vision system. The complexity analysis showed that our proposed technique has the lowest computational time.

and edge wide calculation [12]. The computational complexity of LPC-SI [26] and S3 [14] are determined by the complexity of 2D-FFT which is in the order of $O(n \log(n))$. In BLIINDS, the complexity is identified by the complexity of DCT transform which is in the order of $O(n \log(n))$ by factorizing the

REFERENCES

[1] Z. Wang, A. C. Bovik, H. R. Sheikh, and E. P. Simoncelli, "Image quality assessment: From error visibility to structural similarity," *IEEE Trans. Image Process.*, vol. 13, no. 4, pp. 600–612, 2004.

[2] R. Sheikh, A. C. Bovik, and G. D. Veciana, "An information fidelity criterion for image quality assessment using natural scene statistics," *IEEE Trans. Image Process.*, vol. 14, no. 12, pp. 2117–2128, 2005.

[3] R. Sheikh, M. F. Sabir, and A. C. Bovik, "A statistical evaluation of recent full reference image quality assessment algorithms," *IEEE Trans. Image Process.*, vol. 15, no. 11, pp. 3440–3451, 2006.

[4] R. Sheikh and A. C. Bovik, "Image information and visual quality," *IEEE Trans. Image Process.*, vol. 15, no. 2, pp. 430–444, 2006.

[5] C. Li and A. C. Bovik, "Content-partitioned structural similarity index for image quality assessment," *Signal Process. Image Commun.*, vol. 25, no. 7, pp. 517–526, 2010.

[6] Z. Wang and A. C. Bovik, *Modern Image Quality Assessment*. San Rafael, CA, USA: Morgan and Claypool, 2006.

[7] X. Gao, W. Lu, D. Tao, and X. Li, "Image quality assessment based on multiscale geometric analysis," *IEEE Trans. Image Process.*, vol. 18, no. 7, pp. 1409–1423, 2009.

[8] D. Tao, X. Li, W. Lu, and X. Gao, "Reduced-reference IQA in contourlet domain," *IEEE Trans. Syst., Man, Cybern.*, vol. 39, no. 6, pp. 1623–1627, 2009.

[9] R. Soundararajan and A. C. Bovik, "RRED indices: Reduced reference entropic differencing for image quality assessment," *IEEE Trans. Image Process.*, vol. 21, no. 2, pp. 517–526, 2011.

[10] P. Marziliano, F. Dufaux, S. Winkler, and T. Ebrahimi, "A no-reference perceptual blur metric," in *Proc. ICIP*, 2002, vol. 3, pp. 57–60.

[11] R. Ferzli and L. Karam, "A no-reference objective image sharpness metric based on the notion of just noticeable blur (JNB)," *IEEE Trans. Image Process.*, vol. 18, no. 4, pp. 717–728, 2009.

[12] N. Narvekar and L. Karam, "A no-reference image blur metric based on the cumulative probability of blur detection (CPBD)," *IEEE Trans. Image Process.*, no. 99, pp. 2678–2683, 2011.

[13] S. Varadarajan and L. J. Karam, "An improved perception-based noreference objective image sharpness metric using iterative edge refinement," in *Proc. ICIP*, 2008, pp. 401–404.

[14] C. Vu, T. Phan, and D. Chandler, "S3: A spectral and spatial measure of local perceived sharpness in natural images," *IEEE Trans. Image Process.*, vol. 21, no. 3, pp. 934–945, 2012.

[15] X. Zhu and P. Milanfar, "A no-reference sharpness metric sensitive to blur and noise," in *Proc. QoMEX*, 2009, pp. 64–69.

[16] E. Ong, W. Lin, Z. Lu, S. Yang, S. Yao, F. Pan, L. Jiang, and F. Moschetti, "A no-reference quality metric for measuring image blur," in *Proc. Int. Symp. Signal Process. Appl.*, 2003, vol. 1, pp. 469–472.

[17] A. Mittal, A. Moorthy, and A. Bovik, "No-reference image quality assessment in the spatial domain," *IEEE Trans. Image Process.*, vol. 21, no. 12, pp. 4695–4708, 2012.

[18] F. C. A. Groen, I. T. Young, and G. Ligthart, "A comparison of different focus functions for use in autofocus algorithms," *Cytometry*, vol. 6, pp. 81–91, 1985.

[19] A. Santos, C. O. D. Solorzano, J. J. Vaquero, J. M. Pena, N. Malpica, and F. D. Pozo, "Evaluation of autofocus functions in molecular cytogenetic analysis," *J. Microsc.*, vol. 188, no. 3, pp. 264–272, 1997.

[20] Y. Sun, S. Duthaler, and B. J. Nelson, "Autofocusing in computer microscopy: Selecting the optimal focus algorithm," *Microsc. Res. Techn.*, vol. 65, pp. 139–149, 2004.

[21] H. Tang, N. Joshi, and A. Kapoor, "Learning a blind measure of perceptual image quality," in *Proc. CVPR*, 2011, pp. 305–312.

[22] D. Shaked and I. Tastl, "Sharpness measure: Towards automatic image enhancement," in *Proc. ICIP*, 2005, pp. 937–940.

[23] M. K. Janez and S. Kovacic, "A Bayes-spectral-entropy-basedmeasure of camera focus using a discrete cosine transform," *Pattern Recognit. Lett.*, vol. 27, no. 13, pp. 1431–1439, 2006.

[24] J. Caviedes and F. Oberti, "A new sharpness metric based on local kurtosis, edge and energy information," *Signal Process.: Image Commun.*, vol. 19, no. 2, pp. 147–161, 2004.

[25] M. A. Saad, A. C. Bovik, and C. Charrier, "A perceptual DCT Statistics based blind image quality metric," *IEEE Signal Process. Lett.*, vol. 17, no. 6, pp. 583–586, 2010.

[26] R. Hassen, Z. Wang, and M. Salama, "Image sharpness assessment based on local phase coherence," *IEEE Trans. Image Process.*, vol. 22, no. 7, pp. 2798–2810, 2013.

[27] A. K. Moorthy and A. C. Bovik, "A two-step framework for constructing blind image quality indices," *IEEE Signal Process. Lett.*, vol. 17, no. 5, pp. 513–516, 2010.

[28] A. K. Moorthy and A. C. Bovik, "Blind image quality assessment: From natural scene statistics to perceptual quality," *IEEE Trans. Image Process.*, vol. 20, no. 12, pp. 3350–3364, 2011.

[29] M. Saad, A. Bovik, and C. Charrier, "DCT statistics model-based blind image quality assessment," in *Proc. ICIP*, 2011, pp. 3093–3096.

[30] M. Saad, A. Bovik, and C. Charrier, "Blind image quality assessment: A natural scene statistics approach in the dct domain," *IEEE Trans. Image Process.*, vol. 21, no. 8, pp. 3339–3352, 2012.

[31] L. I. Rudin, S. Osher, and E. Fatemi, "Nonlinear total variation based noise removal algorithms," *Phys. D*, vol. 60, no. 14, pp. 259–268, 1992.

[32] K. Sharifi and A. Leon-Garcia, "Estimation of shape parameter for generalized Gaussian distributions in subband decompositions of video," *IEEE Trans. Circuits Syst. Video Technol.*, vol. 5, no. 1, pp. 52–56, 1995.

[33] H. Sheikh, Z. Wang, L. Cormack, and A. Bovik, LIVE image quality assessment database release 2 [Online]. Available: http://live.ece.utexas.edu/research/quality

[34] N. Ponomarenko, V. Lukin, A. Zelensky, K. Egiazarian, M. Carli, and F. Battisti, "TID2008 - a database for evaluation of full-reference visual quality assessment metrics," *Adv. Mod. Radioelectron.*, vol. 10, no. 4, pp. 30–45, 2009.

[35] E. Larson and D. Chandler, "Most apparent distortion: Full-reference image quality assessment and the role of strategy," *J. Electron. Imag.*, vol. 19, no. 1, pp. 011006-1-011006–21, 2010.

[36] P. L. Callet and F. Autrusseau, Subjective quality assessment IRCCYN/ IVC database 2005 [Online]. Available: http://www.ir-ccyn.ec-nantes.fr/ivcdb/

[37] Final report from the video quality experts group on the validation of objective models of video quality assessment Mar. 2000 [Online]. Available: http://www.vqeg.org/